Journal of Materials Science Research and Reviews

7(4): 15-30, 2021; Article no.JMSRR.66847

Optimization and Modeling of Performance Parameters in Injection Moulding of Plantain Fibre Reinforced High Density Polyethylene (PFRHDPE) for Impact Responses Evaluation

S. P. Obuka Nnaemeka[1*], R. Ozioko Emeka[1] and W. Mba Tochukwu[2]

[1]Department of Mechanical and Production Engineering, Enugu State University of Science and Technology, Enugu, Nigeria.
[2]Department of Postgraduate Studies, African Regional Center for Space Science and Technology, Ile Ife, Osun, Nigeria.

Authors' contributions

This work was carried out in collaboration of the three authors, each contributing to a successful completion of the article. Author SPON was the principal researcher for the research work through which this article was produced. Author ROE was a co-researcher, he carried out the software analysis of the results obtained from the laboratory experiments. While author WMT was the technologist who performed the experiments in the laboratory, hence provided all results for the research.

Article Information

Editor(s):
(1) Dr. Oscar Jaime Restrepo Baena, Universidad Nacional de Colombia, Colombia.
Reviewers:
(1) Felipe Marin, University of the Basque Country, Spain.
(2) Sugiman, University of Mataram, Indonesia.
Complete Peer review History: http://www.sdiarticle4.com/review-history/66847

Original Research Article

Received 23 January 2021
Accepted 31 March 2021
Published 14 April 2021

ABSTRACT

This research work reports the optimization and modeling of injection moulding parameters in the production of plantain fibre particles reinforced high density polyethylene (PFRHDPE) for impact responses evaluation. Composite materials have some limitations, and one of the most significant is their response to localized impact loading. The injection moulding process was designed using Taguchi robust design of experiment. Eight performance parameters were considered as control factors affecting the responses with the volume fraction of the fibre particulates being the only non-machine related parameter. The composite materials produced were prepared with three different particle sizes of the reinforcing plantain particulates. The optimization and modeling process for the

**Corresponding author: Email: nnaemeka.obuka@esut.edu.ng;*

impact responses evaluation was carried out through a classical use of two independent experimental approaches which we named integrated Taguchi-Response Surface Method (TRSM). This TRSM did optimally analyze the ultimate impact strength of plantain fibre particle filled HDPE matrix. The developed second order linear regression models for these composites were significant at the chosen 95% confidence interval, hence showing full response predictability.

Keywords: Impact; injection moulding; optimization; plantain fibres; taguchi-response surface method.

1. INTRODUCTION

Impact is defined as the collision between two or more bodies, where the interaction between the bodies can be elastic, plastic, fluid or any combination of these [1]. When two materials collide with each other at normal speeds, one will absorb most of the impact by deforming and then dispelling the energy in the form of heat and/or sound energy as result of the deformations and vibrations induced in the struck object [2]. After impact event, a series of physical phenomena takes place, such as, elastic, shock, and plastic wave propagation, fracture and fragmentation, perforation, and spallation [3].

Composites are much more susceptible to damage caused by heat and ultra-violet light than metals, these can degrade the resin component by initiating chemical reactions such as oxidation. Though composites are not atmospherically oxidized, but oxidation of resins due to heat damage can reduce the overall strength of composite materials both physical and mechanical strength [4]. Composites have been widely used in aircraft, aerospace, marine, automotive, and oil and gas structures. Composite materials have some limitations, one of the most significant amongst them is their response to localized impact loading.

The capacity for the impact damage resistance of high performance composite materials is one of the most important aspect to be considered in these materials' engineering applications. Impact damage could be expected to occur and could not be ignored , which was induced by the dropped tools, and other objects during transportation and maintenance of composites structures or flying debris during takeoff and landing of aircrafts body, which in recent times are made of composites [5]. The load carrying capacity of composites could be reduced significantly even if the impact damage is undetected by visual inspection. This can lead to decrease in designed allowable strain of the material, hence more attention should be paid to impact and compression after impact of composites.

Composite materials' response to impact loading and the dissipation of the incident energy of the impactor or projectile is very different when compared to metals. The damage zone of a composite is generally complex in nature and very difficult to characterize, hence, the prediction of the post-impact load bearing capability of a damaged composite structure is more difficult than for metals [6]. The complex nature of impact damage of composites has two important consequences;(a) there is no single quantitative descriptor of impact damage and impact resistance measure for composite structures (b) there is no single established testing technique for detecting and quantifying damage mechanisms in composite [7]. However, impact behaviour of composite structures is usually quantified through impact damage resistance (IDR) and impact damage tolerance (IDT).

Fibre reinforced composite materials when subjected to impact loading are capable of absorbing and dissipating large amount of energy in a wide variety of elastic and fracture processes [8,9]. This ability to absorb energy elastically is dependent upon a large number of parameters including, the mechanical properties of both fibres and matrix, the fibre/matrix interfacial strength, the velocity of the impinging projectile and the size of the structural component [10].

2. THEORETICAL OVERVIEW AND APPLICABLE TECHNIQUES

Two classical independent experimental approaches that are usually applied for experimental data optimization are Taguchi robust design and the response surface method. Taguchi robust design uses experimental developed orthogonal array that considers the number of experimental parameters (control or design factors) and noise factors to design a laboratory experiment to optimize a response, considering minimization and maximization. Taguchi approach is limited in the sense that statistical analysis of variance is not applicable and the higher order and interaction effects of

factors are not considered. Above all regression models produced with Taguchi method is not significant. The Taguchi response model for maximization (the greater the better) is expressed as

$$S/_N = -10LOG(MSD) \quad (1)$$

Where

$$MSD = \frac{1}{2}\sum_{i=1}^{n} y_i{}^2 \quad (2)$$

MSD = mean squared deviation, y represents the response of interest, $S/_N$ is the signal-to-noise ratio.

The response surface method fits second order polynomial to response surface, it captures main effects (linear), higher other effects and interaction effects between factors. The method is applicable to statistical analysis of variance. The number of experiments needed for modeling is higher than as needed in Taguchi DOE. The general response model expressed as

$$y = f(x_1, \ x_2, x_3, x_4, \dots \dots x_k) \quad (3)$$

Where

y is the corresponding response, $x_i(1,2,\dots,)$ are coded levels of k quantity process variables.

The Taguchi robust design produces a first-order model with interaction, but adding the interaction term introduces curvature into the response function. Often the curvature in the true response surface is strong enough that the first order model (even with the interaction term included) is inadequate. A second-order model will likely be required in these situations; hence a response surface method of analysis is brought in to complete the optimization process where Taguchi DOE stops.

3. MATERIALS AND APPLICABLE METHODOLOGY

3.1 Materials

The major materials are high density polyethylene obtained from Eleme petrochemical (INDORAMA) and plantain pseudo stem fibres obtained from Akigwe Farms Awa. The fibres are prepared in three particle sizes PS1 (75µm), PS2 (150µm) and PS3 (300µm). Other materials include maleated polyethylene (MAPE) used as a compatibilizer to bring about perfect bonding between the natural fibre and the polymer matrix, Also tensile composite samples were prepared according to ASTM standard for impact plastic composite samples, ASTM D638-02a. While the Charpy impact tests were conducted in accordance with ASTM D6110 standard specifications.

3.2 Formulation and Compounding of Samples

3.2.1 Composition and molding

The acetylated fibres were ground to three particle sizes of standard sieve sizes of 75µm, 150 µm and 300 µm and subsequently the density of fibre was determined according to ASTM D2395. Each of the particle sizes were then compounded with HDPE resin in three volume fractions (10%, 30% and 50%). To each of the compounds were added 3% maleic anhydride grafted PE (MAPE) by weight respectively. The composite samples were then prepared through injection molding using molds developed according to ASTM638 for tensile test. The most important aspect of this section is the composite composition which relates the volume fractions of composite to the weight fraction of composite.

The weight fraction of fibre is related with composite parameters as

$$w_f = \frac{M_f}{M_c} = \frac{\rho_f V_f}{\rho_c V_c} = \frac{\rho_f}{\rho_c} v_f \quad (4)$$

By knowing the mass of composite needed equation (4) becomes very useful for composition.

where,

v_f = volume fraction of fibre, M_f = weight of fibre, M_c = weight of composite, ρ_c = density of composite, many researchers have recommended optimum formulations for different polymer composites of different reinforcements while it is recommended that wood filler of up to 40% weight fraction is appropriate for wood plastic composite(WPC) to be produced through extrusion and injection.

3.2.2 Injection moulding, mould design and clamping force

The mold design of clamping force is carried out to ensure that actual injection force is

established. The ASTM D638-2a specified the cavity projected area which depending on the number of cavities intended to be used, is used in the evaluation of clamping force as expressed in equation (5).

$$Clamping\ Force\ (CF) = Projected\ Area\ of\ Cavity \times \frac{5tons}{in^2} \quad (5)$$

3.3 Design of Experiment (DOE)

The process of design and manufacturing of composite materials always involve experimental procedures which need to be designed for optimum output and response. Design of experiment (DOE) can be highly effective when you wish (a) to optimize product and process designs, study the effect of multiple factors (i.e. variables, parameters, ingredients etc.) on the performance, and solve production problems by objectively laying out the investigative experiments, (b) to study the influence of individual factors on the performance and determine which factor has more influence and which ones have less. DOE using the Taguchi approach has become a much more attractive tool to practicing engineers and scientists in designing and manufacturing of new products and processes, because of its systematic approach to finding optimum values of design factors which lead to economical design with low variability [11].

In order to model and optimize the responses of these our material samples produced through the injection moulding process, the Taguchi L_{18} Orthogonal array was employed. These control variables are basically machine parameters which include; Screw speed, Barrel temperature, Mold temperature, Injection pressure, Holding pressure, Back pressure, Clamping force and of course Fibre volume fraction. Table 1 shows these eight (8) control variables or design factors with their various levels of application for sample formation.

Taguchi DOE and optimization technique has shortcomings as it only identifies the linear effect of factors, while ignoring the quadratic effect and little or no interaction effect. Hence, further analysis and optimization of responses has to be carried out with application of Response Surface Methodology (RSM) for each response. The RSM model includes the linear, quadratic and interaction terms in its expression.

Response surface methodology (RSM) is an assortment of mathematical and statistical techniques that are useful for the modeling and analysis of problems [12]. A response model can be obtained by applying regression analysis and RSM. A second order polynomial is usually applied in fitting a response surface and in the general case; the response surface is represented by (6):

$$y = \beta_0 + \sum_{i=1}^{k} \beta_i x_i + \sum_{i=1}^{k} \beta_{ii} x_i^2 + \sum_{i=1}^{k-1} \sum_{j=2}^{k} \beta_{ij} x_i x_j \quad (6)$$

where, y is the corresponding response, $x_i(1,2,\dots,)$ are coded levels of k quantity process variables, the terms β_0 , β_i , β_{ii} , β_{ij} are second order regression coefficients, the second term in the summation sign in the polynomial equation accounts for linear effects, whereas the third term accounts for higher order effects, the fourth term represents the interactive effects of the process parameters.

For analysis of experimental data, the checking of the adequacy of fit of the model is also necessary, this includes tests for significance of regression model, test of significance of model coefficients and test for lack of fit. Regression analysis is applied to the experimental results to

Table 1. Design factors and levels

S/NO	Design factors	Levels		
		1	2	3
F1	Screw Speed (SS) rpm	20	40	40
F2	Volume Fraction (V_{fr}) %	10	30	50
F3	Barrel Temperature (TB) ^{0}C	150	200	250
F4	Mold Temperature (TM) ^{0}C	30	35	40
F5	Injection Pressure (IP) MPa	70	87.5	105
F6	Holding Pressure (HP) MPa	56	70	84
F7	Back Pressure (BP) MPa	0.4	0.8	1.2
F8	Clamping Force (CF) tons	133	140	147

Table 2. Populated Taguchi L_{18} (2^1 x 3^7) orthogonal array

Exp.	SS (rpm)	V_{fr} (%)	TB (^{O}C)	TM (^{O}C)	IP (MPa)	HP (MPa)	BP (MPa)	CF (tons)
1	20	10	150	30	70	56	0.4	133
2	20	10	200	35	87.5	70	0.8	140
3	20	10	250	40	105	84	1.2	147
4	20	30	150	30	87.5	70	1.2	147
5	20	30	200	35	105	84	0.4	133
6	20	30	250	40	70	56	0.8	140
7	20	50	150	35	70	84	0.8	147
8	20	50	200	40	87.5	56	1.2	133
9	20	50	250	30	105	70	0.4	140
10	40	10	150	40	105	70	0.8	133
11	40	10	200	30	70	84	1.2	140
12	40	10	250	35	87.5	56	0.4	147
13	40	30	150	35	105	56	1.2	140
14	40	30	200	40	70	70	0.4	147
15	40	30	250	30	87.5	84	0.8	133
1 6	40	50	150	40	87.5	84	0.4	140
17	40	50	200	30	105	56	0.8	147
18	40	50	250	35	70	70	1.2	133

find a suitable model and subsequently a desirability function is further applied to obtain optimal response and response variables

The most popular, important and common design available for fitting a second-order model is the central composite design (CCD). It is a design which consists of two-level factorial or fractional factorial chosen as to allow the estimation of all first and second-order and two factor interaction terms augmented with further points which allow pure quadratic effects to be estimated [13,14]. This class of designs was introduced by [15].

However, the analysis of a second-order model is usually cumbersome hence usually carried out using software. In developing the CCD design for our choice 3-level, 8 factor DOE using Minitab 17 statistical software yielded a 90 run central composite design. This invariably, will be costly to execute, therefore we adopted the mixture of Taguchi design of experiment and response surface methodology for our experimental result analysis and optimization, which we termed 'Integrated Taguchi-Response Surface Method' (TRSM).

But, in order to achieve TRSM, the Taguchi DOE experimental data was transformed by fitting multilinear regression model of the form,

$$y = \beta_0 + \beta_1 x_1 + \beta_2 x_2 + \beta_3 x_3 + \beta_4 x_4 + \beta_5 x_5 + \beta_6 x_6 + \beta_7 x_7 + \beta_8 x_8 \quad (7)$$

This model is then transformed by linearization [16] and fitting a power law model of the form,

$$y = \beta_0 \, x_1^{\beta_1} \, x_2^{\beta_2} \, x_3^{\beta_3} \, x_4^{\beta_4} \ldots x_m^{\beta_m} \quad (8)$$

This can be expressed in terms of applicable variables as

$$y = \beta_0 \, SS^{\beta_1} \, Vfr^{\beta_2} \, TB^{\beta_3} \, TM^{\beta_4} \, IP^{\beta_5} \, HP^{\beta_6} BP^{\beta_7} CF^{\beta_8} \quad (9)$$

The power law model of equation (6) will now aid in integrating our experimental data into the responses of the adopted CCD experimental matrix of 90 runs, which implies that the TRSM has been established and thereby can be analyzed linearly.

The response surface model of this study with eight variables is obtained by expansion of equation (6) as

$$\begin{aligned} y &= \beta_0 + \beta_1 x_1 + \beta_2 x_2 + \beta_3 x_3 + \beta_4 x_4 + \beta_5 x_5 + \beta_6 x_6 \\ &+ \beta_7 x_7 + \beta_8 x_8 + \beta_{11} x_1^2 + \beta_{22} x_2^2 + \beta_{33} x_3^2 + \beta_{44} x_4^2 \\ &+ \beta_{55} x_5^2 + \beta_{66} x_6^2 + \beta_{77} x_7^2 + \beta_{88} x_8^2 + \sum_{i=1}^{7} \beta_{i2} x_i x_2 \\ &+ \beta_{i3} x_i x_3 + \beta_{i4} x_i x_4 + \beta_{i5} x_i x_5 + \beta_{i6} x_i x_6 + \beta_{i7} x_i x_7 \\ &+ \beta_{i8} x_i x_8 \end{aligned} \quad (10)$$

The summation of equation (10) is obtained by adding equations (11-17)

For i=1

$$\beta_{12}x_1x_2 + \beta_{13}x_1x_3 + \beta_{14}x_1x_4 + \beta_{15}x_ix_5 + \beta_{16}x_1x_6 + \beta_{17}x_1x_7 + \beta_{18}x_1x_8 \quad (11)$$

For i=2

$$\beta_{22}x_2x_2 + \beta_{23}x_2x_3 + \beta_{24}x_2x_4 + \beta_{25}x_2x_5 + \beta_{26}x_2x_6 + \beta_{27}x_2x_7 + \beta_{28}x_2x_8 \quad (12)$$

For i=3

$$\beta_{32}x_3x_2 + \beta_{33}x_3x_3 + \beta_{34}x_3x_4 + \beta_{35}x_3x_5 + \beta_{36}x_3x_6 + \beta_{37}x_3x_7 + \beta_{38}x_3x_8 \quad (13)$$

For i=4

$$\beta_{42}x_4x_2 + \beta_{43}x_4x_3 + \beta_{44}x_4x_4 + \beta_{45}x_4x_5 + \beta_{46}x_4x_6 + \beta_{47}x_4x_7 + \beta_{48}x_4x_8 \quad (14)$$

For i=5

$$\beta_{52}x_5x_2 + \beta_{53}x_5x_3 + \beta_{54}x_5x_4 + \beta_{55}x_5x_5 + \beta_6x_5x_6 + \beta_{57}x_5x_7 + \beta_{58}x_5x_8 \quad (15)$$

For i=6

$$\beta_{62}x_6x_2 + \beta_{63}x_6x_3 + \beta_{64}x_6x_4 + \beta_{65}x_6x_5 + \beta_{66}x_6x_6 + \beta_{67}x_6x_7 + \beta_{68}x_6x_8 \quad (16)$$

For i=7

$$\beta_{72}x_7x_2 + \beta_{73}x_7x_3 + \beta_{74}x_7x_4 + \beta_{75}x_7x_5 + \beta_{76}x_7x_6 + \beta_{77}x_7x_7 + \beta_{78}x_7x_8 \quad (17)$$

Equation (10) therefore expands to:

$$\begin{aligned} y = {} & \beta_0 + \beta_1x_1 + \beta_2x_2 + \beta_3x_3 + \beta_4x_4 + \beta_5x_5 + \beta_6x_6 + \beta_7x_7 + \beta_8x_8 + \beta_{11}x_1^2 + \beta_{22}x_2^2 + \beta_{33}x_3^2 + \beta_{44}x_4^2 \\ & + \beta_{55}x_5^2 + \beta_{66}x_6^2 + \beta_{77}x_7^2 + \beta_{88}x_8^2 + \beta_{12}x_1x_2 + \beta_{13}x_1x_3 + \beta_{14}x_1x_4 + \beta_{15}x_ix_5 \\ & + \beta_{16}x_1x_6 + \beta_{17}x_1x_7 + \beta_{18}x_1x_8 + \beta_{23}x_2x_3 + \beta_{24}x_2x_4 + \beta_{25}x_2x_5 + \beta_{26}x_2x_6 + \beta_{27}x_2x_7 \\ & + \beta_{28}x_2x_8 + \beta_{32}x_3x_2 + \beta_{34}x_3x_4 + \beta_{35}x_3x_5 + \beta_{36}x_3x_6 + \beta_{37}x_3x_7 + \beta_{38}x_3x_8 + \beta_{42}x_4x_2 \\ & + \beta_{43}x_4x_3 + \beta_{45}x_4x_5 + \beta_{46}x_4x_6 + \beta_{47}x_4x_7 + \beta_{48}x_4x_8 + \beta_{52}x_5x_2 + \beta_{53}x_5x_3 + \beta_{54}x_5x_4 \\ & + \beta_6x_5x_6 + \beta_{57}x_5x_7 + \beta_{58}x_5x_8 + \beta_{62}x_6x_2 + \beta_{63}x_6x_3 + \beta_{64}x_6x_4 + \beta_{65}x_6x_5 + \beta_{67}x_6x_7 \\ & + \beta_{68}x_6x_8 + \\ & + \beta_{11}x_1^2 + \beta_{22}x_2^2 + \beta_{33}x_3^2 + \beta_{44}x_4^2 + \beta_{55}x_5^2 + \beta_{66}x_6^2 + \beta_{77}x_7^2 + \beta_{88}x_8^2 + \beta_{72}x_7x_2 + \\ & \beta_{73}x_7x_3 + \beta_{74}x_7x_4 + \beta_{75}x_7x_5 + \beta_{76}x_7x_6 + \beta_{78}x_7x_8 \end{aligned} \quad (18)$$

4. RESULTS AND DISCUSSION

The composite materials under study were prepared based on three distinct particle sizes of modified plantain fibres in HDPE matrixes produced through injection moulding process according to the Taguchi DOE of Table 2, and impact tests carried out on each of the samples for each experimental run in four (4) replications. The tests were performed at the laboratory of Standard Organization of Nigeria (SON), Enugu. Results of the impact responses for one of the three particle sizes (as an example) are reported in Table 3. For clarity of purpose and understanding of concept, Table 3 should be placed here (i.e. immediately after the above statement).

4.1 Power Law Models of Impact Tests Reports

The power law models of the impact tests on composites of particle sizes 1-3 are as presented in equations (19-21):

$$Y_{Impact\ PS1} = 182515.61SS^{0.0949}Vfr^{0.0590}TB^{-0.0883}TM^{0.1505}\ IP^{-0.1490}HP^{-0.1950}BP^{0.1745}CF^{-1.3358} \quad (19)$$

$$Y_{Impact\ PS2} = 1.3712SS^{-0.0393}Vfr^{0.1356}TB^{0.1151}TM^{-0.6644}IP^{0.3433}HP^{0.3747}BP^{0.0601}CF^{0.4983} \quad (20)$$

$$Y_{Impact\ PS3} = 0.5382SS^{-0.03}Vfr^{0.1615}TB^{0.0988}TM^{-0.1066}IP^{0.1765}HP^{0.1232}BP^{-0.0716}CF^{0.6164} \quad (21)$$

These power law models were obtained through linearization of Taguchi robust design responses (Table 3 as an example) , by the application of equation (7).

4.2 Central Composite Design Matrix of TRSM

The central composite design (CCD) matrix for each of the particle sizes was initiated to obtain fitting for a second order model which could not be obtained through Taguchi application. The results of the analyses conducted using the CCD is shown in Table 4, which is that for particle size 1 as an example. For clarity of purpose and understanding of concept, Table 4 should be placed here (i.e. immediately after the above statement).

4.3 Response Surface Models

The response surface models (RSM) in terms of actual factors of three composite samples of three particle sizes are presented in the following equations for particles sizes 1-3 respectively:

$$\begin{aligned} Y_{PS1} = {} & 353.1 + 1.0048SS + 0.7483Vfr - 0.1429TB + 1.336TM - 0.5289IP - 0.8694HP - 74.686BP \\ & - 2.985CF - 0.004862SS^2 - 0.003882Vfr^2 + 0.000120TB^2 - 0.00508TM^2 + 0.001105IP^2 \\ & + 0.002351HP^2 - 12.254BP^2 + 0.00771CF^2 + 0.000673SS * Vfr - 0.000121SS * TB \\ & + 0.001144SS * TM - 0.000466SS * IP - 0.000807SS * HP + 0.07321SS * BP \\ & - 0.002868SS * CF - 0.000094Vfr * TB + 0.000897Vfr * TM - 0.000361Vfr * IP \\ & - 0.000606Vfr * HP + 0.05303Vfr * BP - 0.002098Vfr * CF - 0.000130TB * TM \\ & + 0.000074TB * IP + 0.000120TB * HP - 0.009968TB * BP + 0.000404TB * CF \\ & - 0.000707TM * IP - 0.001152TM * HP + 0.09549TM * BP - 0.003880TM * CF \\ & + 0.000419IP * HP - 0.03873IP * BP + 0.001499IP * CF - 0.06333HP * BP \\ & + 0.002484HP * CF - 0.21395BP * CF \end{aligned} \quad (22)$$

$$\begin{aligned} Y_{PS2} = {} & 11.4 - 0.2400SS + 0.5771Vfr + 0.0603TB - 1.963TM + 0.3970IP + 0.5394HP + 8.61BP + 0.331CF \\ & + 0.00212SS^2 - 0.007255Vfr^2 - 0.000113TB^2 + 0.04004TM^2 - 0.001296IP^2 \\ & - 0.002104HP^2 - 4.381BP^2 - 0.00052CF^2 - 0.000602SS * Vfr - 0.000124SS * TB \\ & + 0.002343SS * TM - 0.000354SS * IP - 0.000504SS * HP - 0.01574SS * BP \\ & + 0.000278SS * CF + 0.000271Vfr * TB - 0.008666Vfr * TM + 0.001797Vfr * IP \\ & + 0.002453Vfr * HP + 0.03787Vfr * BP + 0.00459Vfr * CF - 0.000951TB * TM \\ & + 0.000195TB * IP + 0.000265TB * HP + 0.00459TB * BP + 0.000171TB * CF \\ & - 0.006322TM * IP - 0.00TM * HP - 0.1331TM * BP - 0.005658TM * CF + 0.001784IP \\ & * HP + 0.02732IP * BP + 0.001101IP * CF + 0.03727HP * BP + 0.001519HP * CF \\ & + 0.02411BP * CF \end{aligned} \quad (23)$$

$$\begin{aligned} Y_{PS3} = {} & 10.5 - 0.07772SS + 0.05214Vfr + 0.0349TB - 0.280TM + 0.1479IP + 0.1288HP - 7.95BP - 0.235CF \\ & - 0.007352Vfr^2 - 0.000082TB^2 + 0.00442TM^2 + 0.000692IP^2 - 0.000783HP^2 \\ & + 5.477BP^2 - 0.00013CF^2 + 0.000243Vfr * TB - 0.001473Vfr * TM + 0.000985Vfr * IP \\ & + 0.000858Vfr * HP - 0.04741fr * BP + 0.002122Vfr * CF - 0.000100TB * TM \\ & + 0.000077TB * IP + 0.000067TB * HP - 0.003692TB * BP + 0.000166TB * CF \\ & - 0.000469TM * IP - 0.000410TM * HP + 0.02127TM * BP - 0.001011TM * CF \\ & + 0.000260IP * HP - 0.01501IP * BP + 0.000652IP * CF - 0.01310HP * BP \\ & + 0.000551HP * CF - 0.03235BP * CF \end{aligned} \quad (24)$$

4.3.1 Optimization and desirability function

The optimum combination of material and injection machine parameters for three particles composites are reported in Table 5 and Figs. 1-3 respectively:

Table 3. Experimental design matrix of Taguchi analysis for impact responses of particle size 1

Exp. Runs	SS (rpm)	Vfr (%)	TB (^{0}C)	TM (^{0}C)	IP (MPa)	HP (MPa)	BP (MPa)	CF (tons)	Mean Response (MPa)
1	20	10	150	30	70	56	0.4	133	72.28
2	20	10	200	35	87.5	70	0.8	140	64.24
3	20	10	250	40	105	84	1.2	147	70.44
4	20	30	150	30	87.5	70	1.2	147	60.60
5	20	30	200	35	105	84	0.4	133	65.90
6	20	30	250	40	70	56	0.8	140	60.87
7	20	50	150	35	70	84	0.8	147	68.63
8	20	50	200	40	87.5	56	1.2	133	73.86
9	20	50	250	30	105	70	0.4	140	67.90
10	40	10	150	40	105	70	0.8	133	76.49
11	40	10	200	30	70	84	1.2	140	71.28
12	40	10	250	35	87.5	56	0.4	147	63.41
13	40	30	150	35	105	56	1.2	140	65.32
14	40	30	200	40	70	70	0.4	147	62.40
15	40	30	250	30	87.5	84	0.8	133	64.78
16	40	50	150	40	87.5	84	0.4	140	65.98
17	40	50	200	30	105	56	0.8	147	66.55
18	40	50	250	35	70	70	1.2	133	67.55

Table 4. Central composite design matrix of TRSM analysis for impact responses of particle size 1

Std order	Run order	Blocks	PtType	SS (rpm)	Vfr (%)	TB (^{0}C)	TM (^{0}C)	IP (MPa)	HP (MPa)	BP (MPa)	CF (tons)	Response Y (MPa)
1	1	1	1	40	50	150	30	105.0	84	1.2	147	96.80725
2	2	1	1	20	10	150	30	105.0	84	1.2	147	82.43296
3	3	1	1	40	10	250	40	105.0	56	0.4	147	78.51458
4	4	1	1	20	10	250	40	70.0	56	1.2	147	94.5971
5	5	1	1	30	30	200	35	87.5	70	0.8	140	96.5637
6	6	1	1	30	30	200	35	87.5	70	0.8	140	96.5637
7	7	1	1	20	10	150	40	70.0	84	0.4	133	86.28456
8	8	1	1	20	50	250	40	70.0	84	0.4	147	79.34537
9	9	1	1	40	50	250	30	70.0	56	0.4	147	87.82868
10	10	1	1	40	10	250	40	105.0	84	0.4	133	82.92281
11	11	1	1	40	10	250	40	70.0	56	0.4	133	95.33435
12	12	1	1	30	30	200	35	87.5	70	1.2	140	103.6434
13	13	1	1	40	10	200	40	70.0	56	1.2	133	120.8082
14	14	1	1	30	30	150	35	87.5	70	0.8	147	90.47097
15	15	1	1	40	10	200	40	70.0	84	0.4	147	77.06375
16	16	1	1	20	10	250	40	105.0	84	1.2	147	82.28155
17	17	1	1	20	50	150	30	105.0	84	0.4	133	85.53502
18	18	1	1	30	30	200	35	105.0	70	0.4	140	85.56264
19	19	1	1	20	50	250	40	105.0	84	0.4	133	85.3779
20	20	1	1	20	50	250	30	87.5	56	1.2	147	93.77535
21	21	1	1	30	30	200	35	105.0	84	0.8	14	93.19091
22	22	1	1	20	50	250	40	105.0	56	0.4	147	80.83916
23	23	1	1	30	30	200	35	70.0	70	0.8	140	99.82826
24	24	1	1	40	50	250	30	105.0	56	0.4	133	94.50619
25	25	1	1	40	10	150	40	70.0	84	1.2	147	97.65557
26	26	1	1	20	10	250	30	105.0	56	0.4	133	80.47357
27	27	1	1	20	10	250	30	70.0	56	0.4	147	74.78757
28	28	1	1	20	10	250	30	105.0	84	0.4	147	65.051
29	29	1	1	30	30	200	35	87.5	70	0.8	140	96.5637
30	30	1	1	40	10	150	30	70.0	84	0.4	147	77.20556

Std order	Run order	Blocks	PtType	SS (rpm)	Vfr (%)	TB (^{0}C)	TM (^{0}C)	IP (MPa)	HP (MPa)	BP (MPa)	CF (tons)	Response Y (MPa)
31	31	2	1	20	50	150	40	70.0	84	1.2	147	100.5469
32	32	2	1	30	30	250	35	87.5	70	0.8	140	94.67968
33	33	2	1	40	50	250	30	105.0	84	0.4	147	76.3943
34	34	2	1	40	10	150	40	105.0	56	1.2	147	99.49408
35	35	2	1	30	30	200	35	87.5	70	0.8	140	96.5637
36	36	2	1	30	30	150	35	87.5	70	0.8	140	99.04807
37	37	2	1	40	50	250	40	105.0	56	1.2	133	119.5387
38	38	2	1	40	10	150	40	105.0	84	1.2	133	105.0802
39	39	2	1	30	30	200	35	87.5	70	0.8	140	96.5637
40	40	2	1	40	10	150	30	105.0	56	0.4	147	78.65907
41	41	2	1	20	10	250	40	105.0	56	1.2	133	101.7892
42	42	2	1	30	30	200	35	87.5	56	0.8	140	100.8582
43	43	2	1	20	50	250	30	70.0	84	1.2	147	92.04252
44	44	2	1	40	10	250	30	105.0	56	1.2	147	91.07878
45	45	2	1	20	10	150	40	105.0	84	0.4	147	71.06144
46	46	2	1	30	50	200	35	87.5	70	0.8	140	99.51831
47	47	2	1	40	50	150	30	105.0	56	1.2	133	119.7587
48	48	2	1	40	50	250	40	105.0	84	1.2	147	96.62943
49	49	2	1	40	50	150	30	70.0	84	1.2	133	117.5458
50	50	2	1	20	10	150	40	70.0	56	0.4	147	81.69762
51	51	2	1	30	30	200	35	105.0	70	0.8	140	93.97577
52	52	2	1	20	50	150	40	105.0	56	1.2	147	102.4398
53	53	2	1	20	10	250	40	70.0	84	1.2	133	99.90829
54	54	2	1	40	10	150	30	105.0	84	0.4	133	83.0754
55	55	2	1	40	50	150	30	70.0	56	1.2	147	111.297
56	56	2	1	20	50	150	30	105.0	56	0.4	147	80.98792
57	57	2	1	40	10	250	30	70.0	84	1.2	147	89.39578
58	58	2	1	30	10	200	35	87.5	70	0.8	140	90.50316
59	59	2	1	20	50	250	30	70.0	56	1.2	133	113.8643
60	60	2	1	20	10	150	30	105.0	56	1.2	133	101.9765
61	61	3	1	20	10	150	40	105.0	56	0.4	133	87.90899
62	62	3	1	40	10	250	30	70.0	56	1.2	133	110.5901

Std order	Run order	Blocks	PtType	SS (rpm)	Vfr (%)	TB (^{0}C)	TM (^{0}C)	IP (MPa)	HP (MPa)	BP (MPa)	CF (tons)	Response Y (MPa)
63	63	3	1	20	10	150	30	70.0	56	1.2	147	94.77118
64	64	3	1	30	30	200	30	87.5	70	0.8	140	94.3507
65	65	3	1	20	50	150	40	70.0	56	1.2	133	124.3849
66	66	3	1	40	50	150	40	70.0	84	0.4	133	101.3305
67	67	3	1	30	30	200	35	87.5	70	0.8	140	96.5637
68	68	3	1	40	10	150	30	70.0	56	0.4	133	95.50978
69	69	3	1	20	50	150	40	105.0	84	1.2	133	108.1913
70	70	3	1	40	50	250	40	70.0	84	1.2	133	117.3298
71	71	3	1	40	50	250	40	70.0	56	1.2	147	111.0925
72	72	3	1	40	30	200	35	87.5	70	0.8	140	99.23631
73	73	3	1	20	50	150	30	70.0	56	0.4	133	98.33754
74	74	3	1	40	10	250	30	105.0	84	1.2	133	96.19243
75	75	3	1	20	50	250	30	105.0	84	1.2	133	99.0404
76	76	3	1	20	50	250	40	70.0	56	0.4	133	98.15691
77	77	3	1	30	30	200	35	87.5	70	0.8	140	96.5637
78	78	3	1	40	50	250	30	70.0	84	0.4	133	92.75985
79	79	3	1	30	30	200	35	87.5	70	0.8	133	103.4119
80	80	3	1	30	30	200	35	87.5	70	0.8	140	96.5637
81	81	3	1	20	30	200	35	87.5	70	0.8	140	92.91864
82	82	3	1	40	50	150	40	105.0	84	0.4	147	83.45282
83	83	3	1	30	30	200	40	87.5	70	0.8	140	98.52261
84	84	3	1	20	10	250	30	70.0	84	0.4	133	78.98654
85	85	3	1	20	10	150	30	70.0	84	1.2	133	100.0921
86	86	3	1	40	50	150	40	105.0	56	0.4	133	103.2382
87	87	3	1	40	50	150	40	70.0	56	0.4	147	95.94369
88	88	3	1	20	50	150	30	70.0	84	0.4	147	79.49139
89	89	3	1	30	30	200	35	87.5	70	0.8	140	96.5637
90	90	3	1	30	30	200	35	87.5	70	0.8	140	96.5637

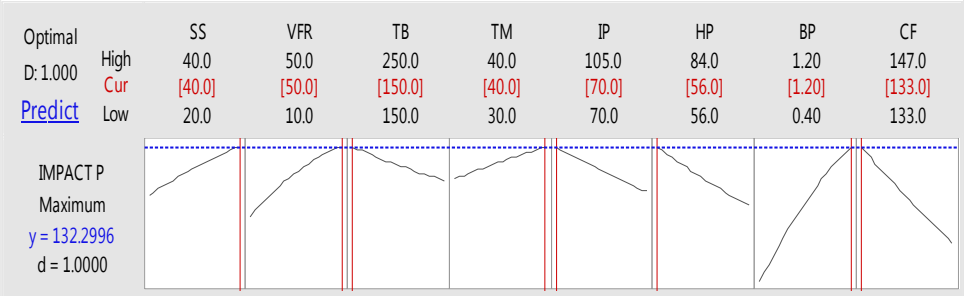

Fig. 1. Optimization plot at full quadratic effects for impact response particle size 1

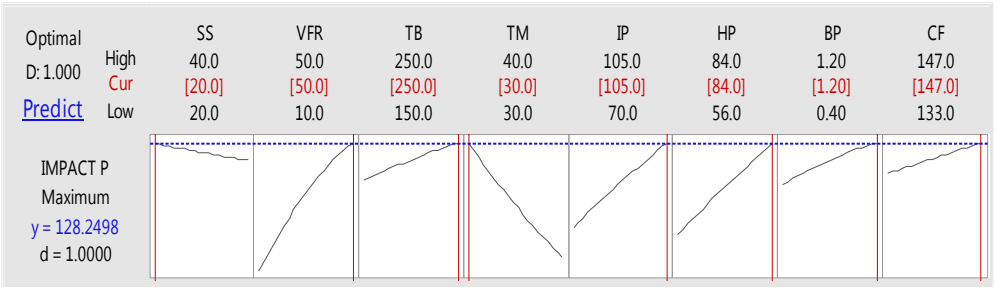

Fig. 2. Optimization plot at full quadratic effects for impact response particle size 2

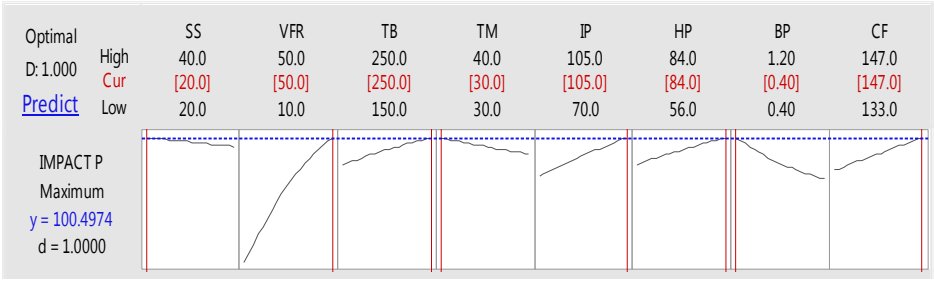

Fig. 3. Optimization plot at refit-full quadratic effects for impact response particle size 3

4.3.2 Response table for optimum production of plantain fibre reinforced HDPE

Optimum performance parameters of material and injection machine parameters are reported in Table 5 for optimum impact strengths of 132.2996 kJ/m^2, 128.2498kJ/m^2 and 100.4974 kJ/m^2 corresponding to three particle sizes.

4.3.3 Regression and analysis of models

Regression analysis is applied to the experimental results to find a suitable model and desirability function is further applied to obtain the optimal processing parameter composition and operating window [17].

Table 6 shows significant effects of main effects, higher order and interaction effects at 95% confidence interval while the fitness of the model was confirmed with the coefficient of determination of 99.99% at full quadratic analysis result of ANOVA. Linear effects showed highest contribution of 98.28% to the tensile response, in which Clamping Force gave the maximum effect to response.

Optimization analysis of impact response particle size 1 (Fig.1, Table 5) showed that at full quadratic effects an optimum impact strength of 132.2996 kJ/m^2 could be obtained at parametric settings of 40rpm of screw speed, 50% volume fraction, 150^{0}C barrel temperature, 40^{0}C mould temperature, 70MPa injection pressure, 56MPa holding pressure, 1.2MPa back pressure, and 133Tonnes clamping force at desirability of 1.000.

Table 5. Response table of optimum material and injection machine parameters

	Optimum setting		
Process Parameter	**PS1**	**PS2**	**PS3**
Screw Speed (SS) rpm	40.00	20.00	20.00
Volume Fraction (V_{fr}) %	50.00	50.00	50.00
Barrel Temperature (TB) ^{0}C	150.00	250.00	250.00
Mold Temperature (TM) ^{0}C	40.00	30.00	30.00
Injection Pressure (IP) MPa	70.00	105.00	105.00
Holding Pressure (HP) MPa	56.00	84.00	84.00
Back Pressure (BP) MPa	1.20	1.20	0.40
Clamping Force (CF) tons	133.00	147.00	147

Table 6. Analysis of variance for 'full quadratic' TRSM design for impact response particle size 1

Source	DF	Seq SS	Adj SS	Adj MS	F-Value	P-Value	Contributions
Model	44	12075.3	12075.3	274.44	29269.90	0.000	99.99%
Linear	8	11868.6	11868.6	1483.57	158228.72	0.000	98.28%
SS (rpm)	1	629.9	629.9	629.89	67180.57	0.000	5.22%
Vfr (%)	1	1310.9	1310.9	1310.93	139815.24	0.000	10.86%
TB (^{0}C)	1	296.5	296.5	296.47	31619.30	0.000	2.46%
TM (^{0}C)	1	272.7	272.7	272.72	29086.33	0.000	2.26%
IP (MPa)	1	531.7	531.7	531.72	56710.29	0.000	4.40%
HP (MPa)	1	910.5	910.5	910.49	97107.08	0.000	7.54%
BP (MPa)	1	5318.1	5318.1	5318.09	567195.25	0.000	44.04%
CF (tons)	1	2598.3	2598.3	2598.27	277115.66	0.000	21.52%
Square	8	123.7	123.7	15.46	1648.73	0.000	1.02%
SS^2 (rpm)	1	101.7	0.5	0.54	57.50	0.000	0.84%
Vfr^2 (%)	1	12.8	5.5	5.50	586.60	0.000	0.11%
TB^2 (^{0}C)	1	0.0	0.2	0.21	21.92	0.000	0.00%
TM^2 (^{0}C)	1	0.3	0.0	0.04	3.93	0.000	0.00%
IP^2 (MPa)	1	0.0	0.3	0.26	27.84	0.000	0.00%
HP^2 (MPa)	1	0.1	0.5	0.48	51.66	0.000	0.00%
BP^2 (MPa)	1	8.5	8.8	8.77	935.03	0.000	0.07%
CF^2 (Tons)	1	0.3	0.3	0.33	34.71	0.000	0.00%
2-Way Interaction	28	83.0	83.0	2.97	316.29	0.000	0.69%
SS*Vfr	1	1.2	1.2	1.16	123.72	0.000	0.01%
SS*TB	1	0.2	0.2	0.23	24.91	0.000	0.00%
SS*TM	1	0.2	0.2	0.21	22.32	0.000	0.00%
SS*IP	1	0.4	0.4	0.42	45.32	0.000	0.00%
SS*HP	1	0.8	0.8	0.82	87.18	0.000	0.01%
SS*BP	1	5.5	5.5	5.49	585.42	0.000	0.04%
SS*CF	1	2.6	2.6	2.58	275.12	0.000	0.02%
Vfr*TB	1	0.6	0.6	0.57	60.42	0.000	0.00%
Vfr*TM	1	0.5	0.5	0.52	54.94	0.000	0.00%
Vfr*IP	1	1.0	1.0	1.02	109,06	0.000	0.01%
Vfr*HP	1	1.8	1.8	1.85	196.85	0.000	0.02%
Vfr*BP	1	11.5	11.5	11.52	1228.56	0.000	0.10%
Vfr*CF	1	5.5	5.5	5.52	588.78	0.000	0.05%
TB*TM	1	0.1	0.1	0.07	7.22	0.010	0.00%
TB*IP	1	0.3	0.3	0.27	28.35	0.000	0.00%
TB*HP	1	0.5	0.5	0.45	48.22	0.000	0.00%
TB*BP	1	2.5	2.5	2.54	271.29	0.000	0.02%
TB*CF	1	1.3	1.3	1.28	136.77	0.000	0.01%

Source	DF	Seq SS	Adj SS	Adj MS	F-Value	P-Value	Contributions
TM*IP	1	0.2	0.2	0.24	26.12	0.000	0.00%
TM*HP	1	0.4	0.4	0.42	44.40	0.000	0.00%
TM*BP	1	2.3	2.3	2.33	248.98	0.000	0.02%
TM*CF	1	1.2	1.2	1.18	125.89	0.000	0.01%
IP*HP	1	0.7	0.7	0.67	71.81	0.000	0.01%
IP*BP	1	4.7	4.7	4.70	501.65	0.000	0.04%
IP*CF	1	2.2	2.2	2.16	230.29	0.000	0.02%
HP*BP	1	8.1	8.1	8.05	858.61	0.000	0.07%
HP*CF	1	3.8	3.8	3.79	404.35	0.000	0.03%
BP*CF	1	23.0	23.0	22.97	2449.54	0.000	0.19%
Error	45	0.4	0.4	0.01			0.00%
Lack of Fit	36	0.4	0.4	0.01			0.00%
Pure Error	9	0.0	0.0	0.0			0.00%
Total	89						

$S = 0.0968304 \quad R^2 = 99.99\% \quad R^2(adj) = 99.98\% \quad PRESS = 2.05713 \quad R^2(pred) = 99.97\%$

The standard deviation of the analysis is 0.0968304 which is close to zero, this implies that the data are clustered very closely around the mean value; hence the response model is reliable. The regression model equation (22) for impact response of particle size 1 show that 99.99% proportion of variance in the dependent variable can be explained by the independent variables. In other words, all the independent variables (main effect) explain or accounts for 99.98% of the variability of the tensile response. This model is also statistically significant with a P-value of 0.000. This indicates that the generated model can statistically predict the tensile strength of our composite.

Similar model for impact response of particle size 2 at refit-full quadratic analysis in 'uncoded' units is obtained as in equation (23). At full quadratic analysis result of ANOVA for impact response particle size 2, the coefficient of determination was 99.98% hence needs no refitting. The ANOVA result also showed that at 95% confidence interval linear effects were completely significant, while in the square effect (higher other effects) only squares of screw speed and clamping force were not significant and only interaction between SS and CF did not show significance at two-way interaction effects Linear effects showed highest contribution of 97.45% to the impact response, in which volume fraction (Vfr) gave the maximum effect to response.

Optimization of impact response of particle size 2 (Fig. 2, Table 5) showed that at full quadratic effects an optimum impact strength of 128.2498 kJ/m^2 could be obtained at parametric settings of 20rpm of screw speed, 50% volume fraction, 250^{0}C barrel temperature, 30^{0}C mould temperature, 105MPa injection pressure, 84MPa holding pressure, 1.2MPa back pressure, and 147Tonnes clamping force at desirability of 1.00.

The standard deviation of the analysis is 0.0759622 which is close to zero, this implies that the data are clustered very closely around the mean value; hence the response model is reliable. The regression model equation for impact response of particle size 2 shows that 99.98% proportion of variance in the dependent variable can be explained by the independent variables. In other words, all the independent variables (main effect) explain or accounts for 99.98% of the variability of the tensile response. This model is also statistically significant with a P-value of 0.000. This indicates that the generated model can statistically predict the dependent variable, Impact strength of our composite.

Unlike those of particle sizes 1 and 2, at full quadratic analysis, ANOVA result for impact response particle size 3 produced a coefficient of determination of 100% which is an indication of saturation, hence the TRSM analysis was refitted. The ANOVA result for refit-full quadratic analysis gave a coefficient of determination of 99.99%. At 95% confidence interval, linear (main) effects were completely significant, while in the square effect (higher order) only squares of mould temperature and clamping force were non-significant and only interaction of HP and BP showed significance at two-way interaction effects. Linear effects (main effects) showed highest contribution of 99.75% to the tensile response, in which Holding Pressure gave the maximum effect of 43.76% to the response amongst the factors.

Optimization analysis of impact response particle size 3 (Fig. 3, Table 5) showed that at refit-full quadratic effects an optimum impact strength of 100.4974 kJ/m^2 could be obtained for particle size 3 at parametric settings of 20rpm of screw speed, 50% volume fraction, 250^{0}C barrel temperature, 30^{0}C mould temperature, 105MPa injection pressure, 84MPa holding pressure, 0.4MPa back pressure, and 147Tonnes clamping force at desirability of 1.00.

The standard deviation of the analysis is 0.129070 which is still close to zero, implies that the data are clustered very closely around the mean value; hence the response model is reliable. The regression model for impact response of particle size 3 shows that 99.99% proportion of variance in the dependent variable can be explained by the independent variables. In other words, all the independent variables (main effect) explain or accounts for 99.99% of the variability of the tensile response. This model is also statistically significant with a P-value of 0.000. This indicates that the generated model can statistically predict the dependent variable, impact strength.

5. CONCLUSION

- Predictive regression models were developed for three particle sizes of plantain fibre reinforced HDPE
- Optimum settings of impact response parameters were established for plantain fibre reinforced HDPE
- Optimum ultimate impact strengths of plantain fibre reinforced HDPE were evaluated as a function of injection machine parameters and volume fraction of fibres,
- The new composite material has an impact strength range of 128 kJ/m^2 to 132 kJ/m^2.
- Integrated Taguchi-Response Surface Method (TRSM) has optimally analyzed the ultimate impact strength of Plantain fibre particle filled thermoplastic HDPE matrix.
- The second order linear regression models developed for these composites were all significant at 95% confidence interval, therefore, they can comfortably predict the impact responses.

ACKNOWLEDGEMENTS

I would like to acknowledge the Petroleum Technology Development Fund (PTDF) whose sponsorship of research on “Design and production of oil and gas facilities using plantain fibres reinforced plastics” lead to this research article publication. Also to be acknowledged are Nnamdi Azikiwe University Awka Nigeria and the Standard Organization of Nigeria (SON) whose laboratories were used for this research.

COMPETING INTERESTS

Authors have declared that no competing interests exist.

REFERENCES

1. Borvik T. An introduction to impact and penetration dynamics. Department of Structural Engineering, Norwegian University of Science and Technology; 2003.
2. Frederick EC, Hagy JL. Factors affecting peak vertical ground reaction forces in running. International Journal of Sport Biomechanics. 1986;2(1):41-49.
3. Meyers MA. Dynamic behaviour of materials. John Wiley and Sons, New York; 1994.
4. Seelenbinder J. Composite heat damage measurement using the handheld Agilent 4100 Exoscan FTIR, easy, non-destructive analysis of large parts. Agilent Technologies, Connecticut, USA; 2011.
5. Zilong Z, Xiaoquan C, Xiaosu Y. An investigation on the impact resistance and residual compressive strength of composite materials. National Key Laboratory of Advanced Composites Materials, Institute of Aeronautical Materials, Beijing, China; 2010.
6. Avery JG. Design manual for impact damage tolerant aircraft structures, AGAR Dograph No 238 NATO; 1981.
7. Minak G, Soskic Z, Pavlovic A, Fragassa C. Characterization of impact behaviour of composite car components. 23rd Nauka 1 Motorna Vozila Science and Motor Vehicles International Automotive Conference with Exhibition, Beograd, Serbia. 2011;1-14.
8. Rilo NF, Ferreira LMS. Experimental study of low-velocity impacts on glass-epoxy laminated composite plates. International Journal of Mechanics and Materials in Design, 2008;4(3):291-300.
9. Cantwell WJ, Morton J. Geometrical effect in the low-velocity impact response of CFRP. Department of Aeronautics,

Imperial College of Science and Technology, London. 1989;12(1): 39-59.
10. Razali N, Sultan MTH, Mustapha F, Yidris N, Ishak MR. Impact damage on composite structure – A review. The International Journal of Engineering and Science, 2014;3(7):8-20.
11. Fowlkes WY, Reveling CM. Engineering methods for robust product design. Addison-Wesley, Reading, Massachusset, USA; 1995.
12. Khan AR. Modeling and optimization of performance characteristics in electrical discharge machining on titanium alloy. Journal of Mechanical Engineering, Transaction of the Mechanical Engineering Division, the Institution of Engineers. 2012;43(3):33-40.
13. Bradley N, Cheng Y. The response surface methodology. A Master's Thesis in Applied Mathematics and Computer Science, Indiana University South Bend; 2007.
14. Akram M, Akhtar M. Central composite designs robust to three missing observations. A. Ph.D. Thesis in Statistics, Islamia University, Bahawalpur; 2002.
15. Box GEP, Wilson KB. On the experimental attainment of optimum conditions (with discussion). Journal of Royal Statistics Society. 1951;B13:1- 45.
16. Chapra SC, Canale RP. Numerical methods for engineers. 5th ed. New York: McGraw-Hill; 2006.
17. Jou YT, Lin WT, Lee WC, Yeh TM. Integrating the Taguchi method and response surface method for process parameter optimization of the injection moulding. Applied Mathematics and Information Sciences: An International Journal. 2014;8(3):1277-1285.

Peer-review history:
The peer review history for this paper can be accessed here:
http://www.sdiarticle4.com/review-history/66847